GMR
The Original

SUSTAINABLE FABRICATION OF MULTISCALE POLYMERIC ELECTROSPUN NANOSCAFFOLDS LOADED WITH CuO NANOPARTICLES FROM *Chondracanthus exasperatus* EXTRACT FOR WOUND HEALING ACTIVITY ON HaCaT KERATINOCYTES CELLS

Sandheep Selvakumar Sunotha[1], Nandha Kumar S[2], Sattanathan Govindharajan[3]*

[1]Saveetha Medical College & Hospital (SMCH), Saveetha Institute of Medical and Technical Sciences (SIMATS), Thandalam, Chennai, Tamil Nadu 602105, India. sandheepselvarks06@gmail.com
[2]Department of Cardiology, Saveetha Medical College and Hospital, Saveetha Institute of Medical And Technical Sciences (SIMATS), Thandalam, Chennai-602105, Tamil Nadu, India. Email: drnandhakumar1@gmail.com
[3]Department of Pathology, Saveetha Medical College and Hospital, Saveetha Institute of Medical And Technical Sciences (SIMATS), Thandalam, Chennai-602105, Tamil Nadu, India. Email: sattanathanphd@gmail.com
*Corresponding Author: sattanathanphd@gmail.com (S.G.).

ABSTRACT
This study reports the green synthesis of copper oxide nanoparticles (CuO NPs) using *Chondracanthus exasperatus* (red marine macroalgae) extract via an ultrasonic-assisted method, followed by their incorporation into starch/polyvinyl alcohol (PVA) electrospun nanoscaffolds for enhanced wound healing applications. UV-Visible spectroscopy confirmed the formation of CuO NPs with a surface plasmon resonance (SPR) peak at 305 nm, while Fourier-transform infrared spectroscopy (FTIR) analysis revealed nanoparticle stabilization through phytochemical interactions. X-ray diffraction (XRD) confirmed the monoclinic crystalline structure of CuO NPs, and Scanning electron microscopy (SEM) demonstrated uniform nanoparticle distribution within nanofibrous scaffolds. Thermogravimetric analysis (TGA) indicated improved thermal stability, and Dynamic light scattering (DLS) /zeta potential analysis confirmed colloidal stability (−22.28 mV). *In vitro* wound healing assays using HaCaT keratinocytes revealed that starch/PVA/CuO-NP nanoscaffolds exhibited superior wound closure rates (97.1% at 100 µg/mL) compared to CuO NPs (85.1%) and algal extract (71.1%), highlighting their potential as bioactive wound dressings. These findings suggest that the phytochemically synthesized CuO NPs embedded in starch/PVA nanofibers offer a biocompatible, thermally stable, and highly effective scaffold for accelerating wound regeneration.

KEYWORDS: *Chondracanthus exasperatus*, Green synthesis, CuO nanoparticles, starch/PVA nanoscaffolds, Wound-healing activity.

1. INTRODUCTION

Wound healing is an intricate biological process involving a coordinated cascade of cellular and molecular events that restore the skin's structural integrity and function following injury [1]. This multifaceted process encompasses hemostasis, inflammation, proliferation, and tissue remodeling, which are vulnerable to disruption under various pathological conditions such as infections, diabetes, and oxidative stress [2]. Chronic wounds pose a significant global health challenge, often leading to prolonged hospital stays, increased healthcare costs, and reduced quality of life [3]. In this context, the development of innovative, biocompatible wound dressings capable of accelerating tissue regeneration while offering antimicrobial protection has become a priority in biomedical research [4].

Nanotechnology has emerged as a promising tool in regenerative medicine due to its capacity to engineer materials at the nanoscale, providing unique physicochemical and biological properties [5]. Among the various nanomaterials investigated, metal oxide nanoparticles—especially copper oxide nanoparticles (CuO NPs)—have drawn considerable attention owing to their intrinsic antimicrobial, antioxidant, and wound-healing capabilities [6]. Copper is an essential trace element that plays a vital role in angiogenesis, collagen synthesis, and re-epithelialization [7]. Its incorporation into wound dressings has been shown to enhance cellular proliferation and reduce microbial load at the wound site [8]. However, traditional chemical and physical methods of synthesizing CuO NPs often involve hazardous reagents, high energy consumption, and the generation of toxic byproducts, making them less suitable for biomedical applications [9].

To overcome these limitations, green synthesis approaches have been increasingly adopted for nanoparticle production [10]. These eco-friendly methods utilize biological resources such as plant extracts, microbes, or marine algae, which act as both reducing and capping agents [11]. Marine macroalgae, in particular, have emerged as excellent candidates for green nanoparticle synthesis due to their rich phytochemical content, including polyphenols, flavonoids, terpenoids, and sulfated polysaccharides [12]. These bioactive compounds not only

facilitate metal ion reduction but also enhance the stability and biological efficacy of the resulting nanoparticles [13].

Chondracanthus exasperatus, a species of red marine macroalgae, is abundant along the southern coast of India and is known for its diverse phytochemical profile and medicinal properties [14]. Despite its potential, its application in nanobiotechnology remains largely underexplored [15]. This study harnesses the biomolecular constituents of *C. exasperatus* for the green synthesis of CuO NPs via an ultrasonic-assisted extraction method, which improves the yield and bioavailability of active compounds [16]. Ultrasonication promotes cell disruption and enhances solvent penetration, facilitating efficient extraction of phytochemicals necessary for nanoparticle formation [17].

Once synthesized, the CuO NPs were incorporated into electrospun nanofibrous scaffolds composed of starch and polyvinyl alcohol (PVA) [18]. Electrospinning is a well-established technique for fabricating nanofibrous matrices that closely mimic the extracellular matrix (ECM) of human tissues [19]. These nanofibers offer high surface area, tunable porosity, and excellent mechanical properties, making them ideal for wound dressing applications [20]. PVA, a synthetic polymer widely used in biomedical fields, provides structural integrity and ease of electrospinning, while starch, a natural polysaccharide, contributes to the biocompatibility and biodegradability of the scaffold [21]. The blend of PVA and starch thus creates a synergistic matrix that can support controlled nanoparticle release, moisture retention, and cell adhesion—critical features for efficient wound management [22].

The integration of biogenically synthesized CuO NPs into starch/PVA nanofibers aims to create a multifunctional wound dressing with enhanced antimicrobial activity, biocompatibility, and regenerative potential [23]. The nanoparticles confer antibacterial and anti-inflammatory properties, while the scaffold provides a conducive environment for cellular activities such as migration and proliferation [24]. Moreover, the green synthesis process ensures that the scaffold is free from cytotoxic residues typically associated with chemically synthesized nanoparticles, thereby improving safety and efficacy in biomedical applications [25].

To validate the material's suitability for wound healing, comprehensive physicochemical characterizations were conducted [26]. UV–visible spectroscopy confirmed nanoparticle formation via distinct absorption peaks associated with surface plasmon resonance [27]. Fourier transform infrared (FTIR) spectroscopy revealed functional groups involved in the reduction and stabilization processes [28], while X-ray diffraction (XRD) analysis confirmed the crystalline nature of the CuO NPs and their incorporation into the fiber matrix [29]. Scanning electron microscopy (SEM) provided insights into the surface morphology and fiber uniformity, confirming successful electrospinning of nanoparticle-embedded nanofibers [30]. Thermogravimetric analysis (TGA) demonstrated the scaffold's enhanced thermal stability, indicating its robustness under physiological conditions [31]. Dynamic light scattering (DLS) and zeta potential measurements further corroborated the nanoscale size distribution and colloidal stability of the CuO particles, affirming their biomedical compatibility [32].

To assess the biological efficacy of the fabricated nanoscaffolds, an *in vitro* scratch assay using human keratinocyte (HaCaT) cells was performed [33]. This assay provides a reliable model to evaluate cell migration and wound closure—two critical parameters in the wound healing process [34]. The results indicated that the starch/PVA/CuO nanoscaffolds significantly accelerated cell migration compared to untreated controls and individual components, highlighting their potential as advanced wound healing materials.

2. MATERIALS AND METHODS

2.1 Reagents and raw materials

C. exasperatus, a brown algal species sourced from the coastal region of Rameswaram, Tamil Nadu, was used as a natural reductant for synthesizing CuO NPs. This alga is rich in bioactive phytoconstituents capable of metal ion reduction. Analytical-grade copper (II) sulfate pentahydrate (Merck, Germany) served as the metal precursor. For nanofiber synthesis, PVA (molecular weight ~115,000 g/mol) and starch were employed. PVA was selected due to its excellent electrospinning behavior and biocompatibility, while starch contributed to fiber degradability and enhanced composite performance with synthetic polymers. HaCaT keratinocytes cells were obtained from the National Centre for Cell Science (NCCS), Pune, India, which provided authenticated and contamination-free cell stocks for biological investigations focused on wound healing activity.

2.2 Algal biomass collection and preparation

Fresh *C. exasperatus* specimens were hand-harvested from the intertidal regions of Rameswaram. The collected *C. exasperates* was taxonomically identified and authenticated by Dr V. Veeragurunathan, CSIR-CSMCRI-Marine Algal Research Station, Mandapam Camp 623519, Tamil Nadu, India. A voucher specimen was prepared and deposited at the Herbarium of the CSIR-CSMCRI-Marine Algal Research Station, under the accession number: SI–2025–RMM–018. This authentication ensures botanical accuracy and standardization of the study material. To preserve the integrity of active compounds, samples were kept chilled in sterile containers during transport to the lab. In the laboratory, the algae were rinsed thoroughly with tap water to remove surface impurities, followed by distilled water to eliminate any remaining salts. Around 100 g of the cleaned sample was chopped and shade-dried at 28 ± 2°C for two weeks. The dried algae were pulverized into powder, sieved for uniformity, and stored in airtight, moisture-resistant containers until use.

2.3 Ultrasonic-assisted extraction of bioactives

Bioactives were extracted using ultrasonic-assisted extraction (UAE), enhancing the release of intracellular compounds. Two grams of powdered algal biomass were dispersed in 50 mL of Milli-Q water in a 100 mL borosilicate beaker and subjected to sonication at 60°C for 45 minutes using a LABQUEST ultrasonic bath (Borosil, Serial No. 941032329018). The mixture was then filtered through Whatman No. 1 filter paper. The resultant clear extract, rich in phenolic compounds, flavonoids, and polysaccharides, was either used fresh or refrigerated at 10°C. A portion was freeze-dried and stored for long-term applications [35, 36].

2.4 Biosynthesis of CuO NPs

The synthesis of CuO NPs was initiated by slowly adding 10 mL of the algal extract (10 mg/mL concentration) into 50 mL of 0.1 M copper sulfate under constant stirring at 650 rpm and 60°C for two hours, maintaining a 5:1 volume ratio (salt to extract). A visible color change from blue to bluish-green signaled the reduction of Cu^{2+} ions. The nanoparticles were recovered via centrifugation, washed three times with distilled water, and freeze-dried for 48 hours to obtain a dry nanopowder suitable for incorporation into nanofiber scaffolds [37].

2.5 Electrospinning of CuO-embedded nanofibers

An aqueous solution of PVA at 15% (w/w) was prepared by continuous stirring at 50°C until completely dissolved. Following this, 100 mg each of starch and synthesized CuO NPs were added and stirred for 2.5 hours to ensure a uniform mixture. The solution was loaded into a 10 mL syringe fitted with a stainless-steel needle of 0.84 mm internal diameter. Electrospinning was carried out using a HOLMARC HO-NFES-040 setup at 11.5 kV, with a flow rate of 0.4 mL/h and a tip-to-collector distance of 12.3 cm. The process lasted for 6–8 hours at 25 ± 2°C. Nanofibers were collected on aluminum foil and preserved in a desiccated environment [38-40].

2.6 Characterization of synthesized materials

2.6.1 UV–visible spectroscopy

The formation and optical features of CuO NPs were evaluated using a VIS SPEC V-730 UV–Visible spectrophotometer over a wavelength range of 200–800 nm, with deionized water as the blank. The presence of characteristic absorbance peaks between 270–300 nm confirmed nanoparticle formation due to surface plasmon resonance (SPR) effects [41].

2.6.2 FTIR spectroscopic analysis

FTIR spectroscopy was conducted using a PerkinElmer Spectrum Two spectrometer in ATR mode. Scans were recorded over the range of 4000–400 cm^{-1} at 4 cm^{-1} resolution and 64 accumulations. Key bands corresponding to O–H, C=O, N–H, and Cu–O confirmed the involvement of bioactives in nanoparticle formation and their successful integration into the fiber matrix [42].

2.6.3 XRD analysis

The crystalline characteristics of synthesized CuO and nanofibers were studied using a Bruker D8 Advance X-ray diffractometer with CuKα radiation (λ = 1.5406 Å), operated at 40 kV and 40 mA. Scans were performed over a 2θ range from 5° to 90° at a step size of 0.029649°. Sharp peaks indicated the monoclinic structure of CuO, while broadened patterns in composite fibers suggested effective incorporation [43].

2.6.4 SEM analysis

The surface architecture of nanofibers was assessed via SEM using a JEOL JSM-IT800 NANO instrument. Samples were sputter-coated with gold to improve conductivity. The SEM micrographs exhibited continuous, bead-free fibers with homogeneous distribution of CuO NPs throughout the scaffold [44].

2.6.5 TGA

Thermal stability of the fibers was investigated using a PerkinElmer TGA 8000 analyzer. Approximately 5 mg of each sample was placed in aluminum crucibles and heated from ambient temperature to 550°C at a rate of 15°C/min under nitrogen flow. TGA profiles showed distinct phases of water loss, polymer degradation, and residual mass, with CuO-enhanced fibers demonstrating superior thermal resistance [45].

2.6.6 DLS and zeta potential

DLS and zeta potential measurements were carried out using a Malvern Zetasizer Ultra to determine nanoparticle size and colloidal stability. The particle size distribution confirmed nano-range dimensions, and zeta potential values (≥ ±30 mV) indicated high stability, affirming their applicability in biomedical systems [29]. All relevant raw and processed datasets are archived in Mendeley Data (DOI: 10.17632/99bn3x4yzb.2).

2.7 Wound healing (scratch) assay

The scratch assay was employed to examine the migration ability of HaCaT keratinocytes treated with algal extract, CuO NPs, and PVA/starch/CuO composite fibers. Cells were seeded in 12-well plates at a density of 2×10^5 cells/well using DMEM supplemented with 10% FBS and 1% penicillin-streptomycin and incubated at 37°C with 5% CO_2 until confluent. A sterile 200 µL pipette tip was used to create a central linear scratch. Wells were rinsed with PBS to remove debris, and cells were exposed to test samples at concentrations of 6.25, 12.5, 25, 50, and 100 µg/mL in serum-free DMEM. Untreated controls were also maintained. Microscopic images were taken at 0, 24, and 48 hours using an inverted phase-contrast microscope, and wound closure was quantified using ImageJ software to evaluate cell migration and healing efficiency [46].

2.8 Statistical analysis

All experimental data were statistically evaluated using SPSS version 25.0 and GraphPad Prism version 9.0. Results from triplicate experiments were expressed as mean ± standard deviation. One-way analysis of variance (ANOVA), followed by Tukey's or Dunnett's multiple comparison tests, was used to detect significant differences among groups. A p-value less than 0.05 indicated significance. Pearson's correlation assessed associations among variables. The Shapiro–Wilk test was employed to verify normal distribution, with non-normal datasets subjected to logarithmic transformation. All analyses were performed with a 95% confidence interval [47].

3. RESULTS AND DISCUSSION

3.1. UV-visible spectroscopy

The successful green synthesis of CuO NPs using *C. exasperatus* extract was validated through UV-Visible spectrophotometric analysis (Fig. 1). The algal extract demonstrated a broad absorbance in the range of 200–400 nm, a feature commonly linked to the presence of polyphenolic and flavonoid constituents, with a distinct absorption peak observed at 267 nm, attributed to $\pi \rightarrow \pi^*$ electronic transitions within aromatic ring systems. The biosynthesized CuO NPs exhibited a distinct surface plasmon resonance (SPR) peak at 305 nm, signifying the presence of localized collective oscillations of conduction electrons upon light excitation—an optical hallmark of CuO NPs. The shift in peak from the typical CuO wavelength near 350 nm towards a lower wavelength (blue shift) indicates the formation of uniformly distributed nanoscale particles. The lack of absorption beyond 400 nm confirms the minimal agglomeration of the nanoparticles. The spectral distinction between the peak of the extract (267 nm) and the SPR band of CuO (305 nm) supports the complete reduction of Cu^{2+} ions to CuO. Furthermore, the flat spectral profile beyond 500 nm implies negligible scattering of light, suggesting excellent colloidal stability. These spectral attributes align with existing research on plant-mediated CuO NP synthesis, reinforcing that the ultrasound-assisted extraction (UAE) method facilitated the efficient and uniform formation of stable CuO NPs [48-53].

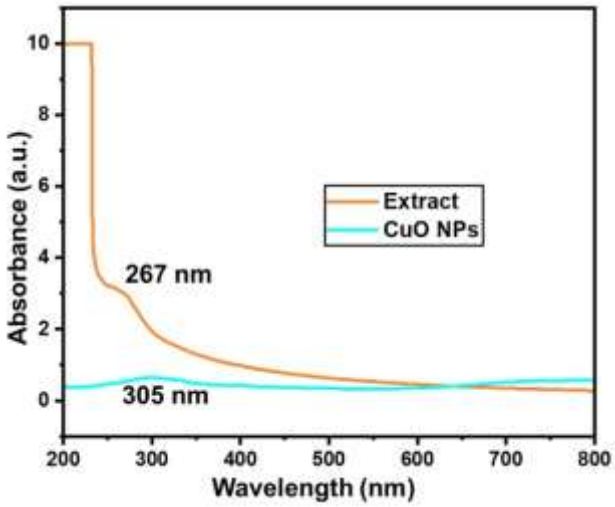

Fig. 1. UV–Visible spectral profiles of algal extract and CuO NPs.

3.2. FTIR spectroscopic analysis

FTIR spectroscopic analysis confirmed the biosynthesis of CuO NPs and their successful incorporation into starch/PVA-based nanofibrous scaffolds (Fig. 2). The FTIR spectrum of CuO NPs exhibited eight prominent absorption bands, including a broad O–H stretch (3200–3400 cm^{-1}), indicating the presence of hydroxyl groups from phenolic or alcoholic compounds, a strong C=O stretch at 1635 cm^{-1} suggesting organic residues, and a characteristic Cu–O bond vibration at 510 cm^{-1} affirming nanoparticle formation. In contrast, the FTIR profile of the nanocomposite scaffolds displayed seven peaks, such as those at 3280 cm^{-1} (O–H), 2920 cm^{-1} (C–H), and 1020 cm^{-1} (C–O–C), signifying the structural features of the polymer matrix. The disappearance of the extract's typical carbonyl peak at 1740 cm^{-1} and the appearance of a new band at 620 cm^{-1} imply a possible coordination interaction between CuO NPs and PVA chains. The reduction from eight to seven bands also suggests a molecular reconfiguration triggered by the electrospinning process. The continued presence of the Cu–O vibration band indicates that the nanoparticles retained their structural integrity during scaffold formation. Overall, the FTIR findings confirm (1) nanoparticle stabilization through phytochemical encapsulation, (2) strong hydrogen bonding interactions between starch and PVA, and (3) effective CuO-polymer integration, which is critical for achieving a cohesive and functional nanofibrous scaffold [54-59].

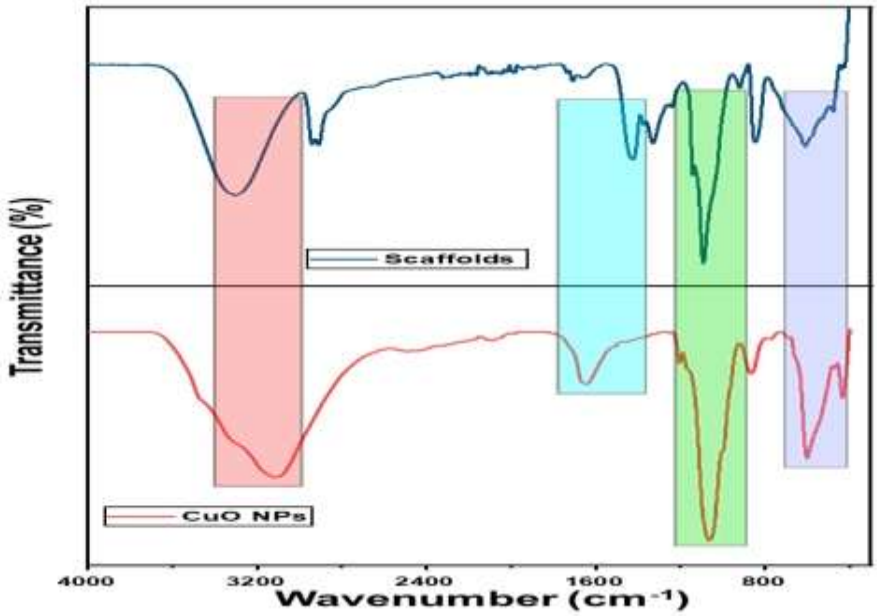

Fig. 2. FTIR spectra of CuO NPs and their incorporation into nanoscaffolds.

3.3. XRD analysis

XRD analysis (Fig. 3) demonstrated the crystalline structure of biosynthesized CuO NPs and their distribution within the starch/PVA nanofiber composite. The CuO NPs produced 32 diffraction peaks across a 2θ range of 12.852° to 57.087°, with major reflections at 19.003° (d-spacing: 4.666 Å), 24.173° (d = 3.679 Å), and 27.314° (d = 3.262 Å), corresponding to the monoclinic crystalline form of tenorite CuO (JCPDS No. 48-1548). The high crystallinity index of 51.1% and narrow full-width at half maximum (FWHM) values (0.100°–0.713°) reveal the formation of highly ordered nanocrystals. XRD patterns of the composite scaffold revealed 13 peaks, including dominant ones at 29.445° (d = 3.031 Å) and 21.420° (d = 4.145 Å), indicative of a reduced crystallinity (20.2%) due to polymer blending. The peak broadening in the scaffold spectrum (FWHM 0.139°–0.579°) is consistent with the homogeneous dispersion of nanoparticles within the polymer matrix. Emergence of new peaks at 36.146° and 47.338° suggests interactions between CuO and PVA chains. Notably, the absence of any impurity peaks supports the high purity of the composite, while peak shifts such as the transition from 35.297° to 35.998° point toward robust interfacial bonding between nanoparticles and polymeric components. These structural insights confirm that the CuO NPs are not only well-incorporated into the matrix but also maintain their monoclinic framework, vital for their functional performance [60-64].

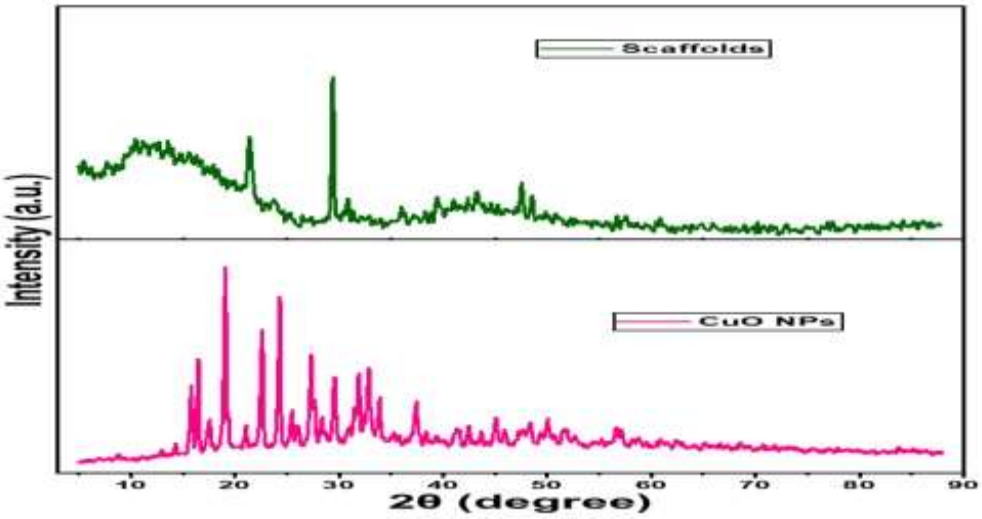

Fig. 3. XRD patterns of synthesized CuO NPs and CuO-loaded scaffolds.

3.4. SEM analysis

SEM analysis (Fig. 4) provided insight into the morphological characteristics of both CuO NPs and the electrospun starch/PVA nanofibrous scaffold. The synthesized CuO NPs appeared as nearly spherical particles, measuring between 100 and 200 nm, with smooth surfaces and limited particle agglomeration, suggesting efficient stabilization by phytochemicals present in the algal extract. The electrospun nanofibers were uniform and devoid of beads, with diameters ranging from 100 to 150 nm. These nanofibers formed a well-porous, interconnected

network structure, which is essential for applications in tissue engineering and regenerative medicine. High-resolution imaging showed that CuO NPs were evenly distributed and embedded along the surface of the nanofibers. The incorporation of nanoparticles resulted in only minor surface roughness, while the structural integrity of the scaffold remained largely intact. Energy dispersive X-ray spectroscopy (EDS) mapping revealed a uniform distribution of copper throughout the scaffold. Compared to control fibers without nanoparticles, over 90% of the morphological characteristics were retained post-incorporation. Furthermore, the slightly roughened surface introduced by nanoparticle inclusion is likely to enhance cellular adhesion. These findings underscore that the applied electrospinning conditions facilitated even nanoparticle dispersion while maintaining the scaffold's overall morphological fidelity [65-69].

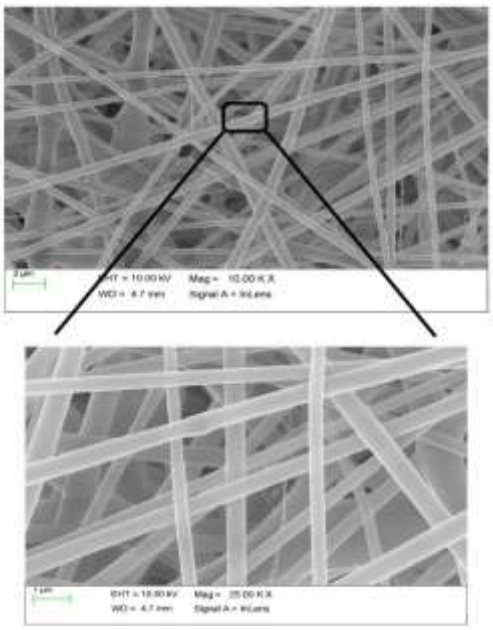

Fig. 4. SEM analysis of synthesized CuO NPs and CuO-loaded scaffolds

3.5. TGA analysis

TGA, conducted under nitrogen flow (Fig. 5), demonstrated that the incorporation of CuO NPs improved the thermal resistance of the starch/PVA scaffolds. The thermal degradation occurred in three distinct phases. The first weight loss, around 8.36%, occurred below 150°C and was attributed to the evaporation of surface-adsorbed moisture associated with hydrophilic groups in the polymers. The second phase began at 252.14°C and reached a maximum rate at 334.73°C (−3.08%/min), corresponding to the decomposition of starch's glycosidic bonds and PVA chains. The final degradation phase peaked at 441.57°C (−2.87%/min), attributed to the breakdown of the main polymeric backbone. The residual mass at 550°C was 35.00%, which was significantly higher than in the control scaffolds, indicating that CuO NPs reinforced the polymeric matrix. Shifts in derivative thermogravimetric (DTG) peaks by 45.91°C and 104.2°C compared to unmodified scaffolds suggest that CuO nanoparticles functioned both as a thermal stabilizer and as a catalyst for char formation through metal-polymer interaction. These thermal behaviors demonstrate that the scaffold is thermally stable up to 250°C and the final residue is consistent with the expected CuO content, confirming uniform nanoparticle dispersion throughout the material [70-74].

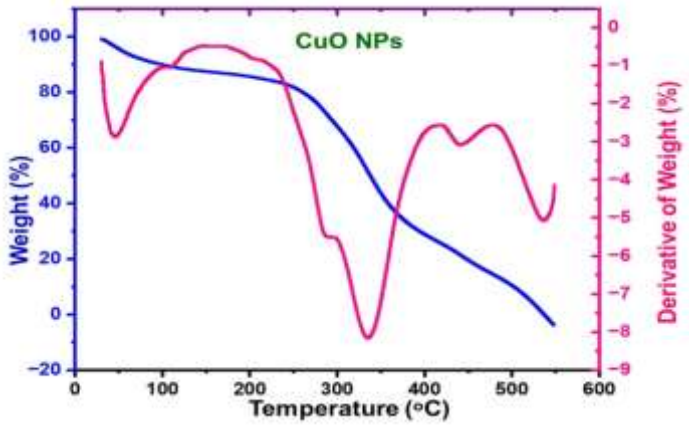

Fig. 5. Thermal degradation behavior of CuO-incorporated nanoscaffolds.

3.6. Zeta potential and particle size analysis

DLS analysis revealed that the green-synthesized CuO NPs exhibited a trimodal size distribution, with a Z-average particle diameter of 169.9 nm and a polydispersity index (PDI) of 0.615, indicating moderate heterogeneity in particle size (Fig. 6). Approximately 98.26% of the measured particles were under 2 µm in diameter, suggesting an overall monodisperse system with minimal agglomeration. Zeta potential measurements showed an average surface charge of −22.28 mV, with prominent peaks at −30.12 mV and −18.58 mV (Fig. 7), likely resulting from varied phytochemical coverage on nanoparticle surfaces. The higher negative zeta potential peak (−30.12 mV) suggests strong electrostatic repulsion forces, which contribute to the colloidal stability of the nanoparticle suspension. Measurement accuracy was confirmed by high DLS intensity count rates (6040 kcps) and zeta count rates (161,500 kcps), along with an intercept value of 0.822. Additionally, a wall potential of −10.04 mV indicated minimal sample interaction with the cuvette surface. Altogether, these data affirm the synthesis of environmentally benign, stable, and moderately monodisperse CuO NPs, suitable for biomedical applications that demand reliable nanoparticle-biological interface behavior [75, 76].

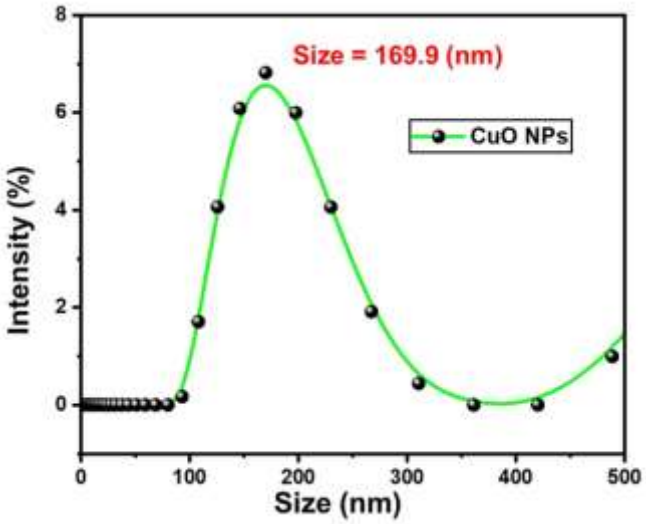

Fig.6. DLS particles size analysis of CuO NPs

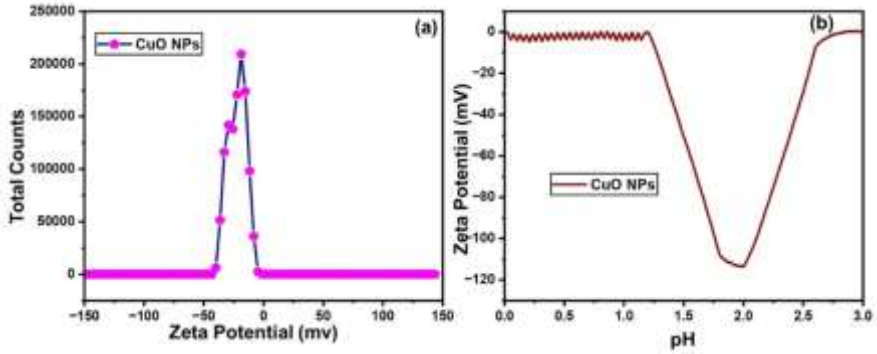

Fig.7. Zeta-potential analysis of CuO NPs

3.7. Wound healing (scratch) assay

The wound healing assay (Fig. 8) demonstrated significant variations in the migratory behavior of HaCaT keratinocyte cells after 48 hours of treatment with algal extract, CuO NPs, and starch/PVA/CuO-NPs nanoscaffolds. At the lowest concentration (6.25 µg/mL), the algal extract exhibited a wound closure rate of 34.10%, while CuO NPs and nanoscaffolds showed higher closure rates of 42.10% and 49.10%, respectively. This indicates that the nanoscaffolds and CuO NPs were more effective in promoting cell migration compared to the algal extract at this concentration.

As the concentration increased to 12.5 µg/mL, the algal extract improved wound closure to 41.10%, whereas CuO NPs and nanoscaffolds further enhanced closure to 48.10% and 64.10%, respectively. The nanoscaffolds continued to outperform the other treatments, suggesting their superior ability to facilitate keratinocyte migration. At 25 µg/mL, the algal extract achieved 52.10% wound closure, while CuO NPs and nanoscaffolds reached 64.10% and 75.10%, reinforcing the trend of nanoscaffolds exhibiting the highest efficacy.

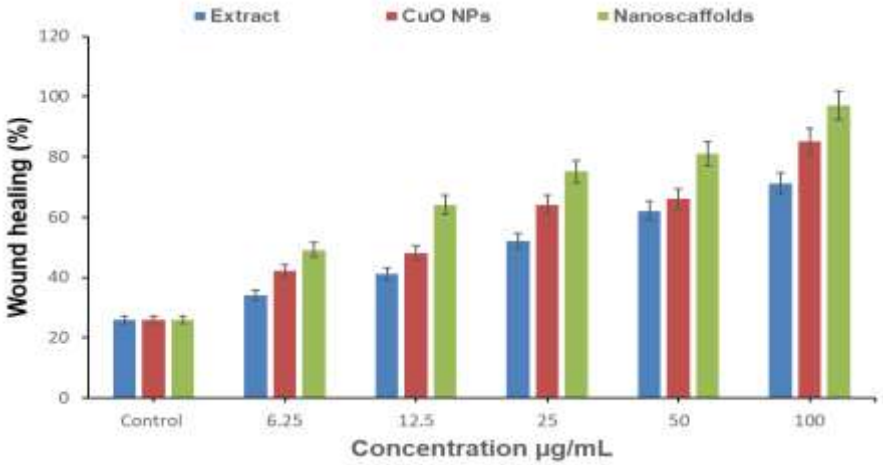

Fig. 8. Wound healing activity analysis of algal extract, CuO-NPs and starch/PVA/CuO-NPs nanoscaffolds

Higher concentrations (50 µg/mL and 100 µg/mL) further highlighted the differences in performance. The algal extract resulted in 62.10% and 71.10% wound closure, respectively, while CuO NPs showed 66.10% and 85.10% closure. Notably, the nanoscaffolds achieved the most substantial wound healing, with closure rates of 81.10% and 97.10% at these concentrations. This suggests that the starch/PVA/CuO-NPs nanoscaffolds possess the strongest pro-migratory effects, likely due to their composite structure, which may enhance cell adhesion and proliferation.

Collectively, the wound healing assay revealed that all test samples promoted keratinocyte migration, but the starch/PVA/CuO-NPs nanoscaffolds consistently exhibited the highest wound closure rates across all concentrations. CuO NPs also demonstrated strong activity, while the algal extract, though effective, had comparatively lower efficacy. These findings highlight the potential of nanoscaffolds as a promising therapeutic agent for wound healing applications [77-79].

4. CONCLUSION

This study successfully demonstrated the green synthesis of stable, phytochemically capped CuO NPs using *C. exasperatus* extract via an ultrasonic-assisted approach, followed by their incorporation into starch/PVA electrospun nanoscaffolds for enhanced wound healing applications. Comprehensive characterization confirmed the formation of monoclinic CuO NPs (UV-Vis, XRD), their successful integration into nanofibers (SEM, FTIR), and improved thermal stability (TGA). The nanoscaffolds exhibited a highly porous, interconnected structure with uniform nanoparticle distribution, essential for cell adhesion and proliferation. *In vitro* wound healing assays revealed that the starch/PVA/CuO-NP nanoscaffolds outperformed both free CuO NPs and algal extract, achieving near-complete wound closure (97.1% at 100 µg/mL) due to their bioactive and structural advantages. The negative zeta potential (−22.28 mV) further confirmed colloidal stability, minimizing aggregation risks. These findings highlight the scaffold's potential as a biocompatible, thermally stable, and functionally efficient wound dressing that accelerates tissue regeneration. Future studies should explore *in vivo* efficacy and long-term biocompatibility to validate clinical applicability.

Ethics declaration: Not Applicable

Funding Declaration: Not Available for this study

Conflicts of Interest: The authors declare no conflicts of interest.

Data Availability Statement: The full dataset of physiochemical characterization associated with this work is published in Mendeley Data [Dataset] Structural and functional profiling of starch-polymer nanoscaffolds enhanced with Ectocarpales-derived biogenic copper oxide nanoparticles (DOI: 10.17632/m7jzmb7mr9.1). Disclosure: The material characterization data and figures (e.g., UV, SEM, FTIR, XRD, TGA, Zeta Potential and particle sizer) presented here were generated from a common dataset and are being reused across multiple related studies on nanomaterials. All biological analyses and conclusions are original to each manuscript.

REFERENCES

[1] Perumal MKK, Renuka RR, Subbiah SK, Natarajan PM. Artificial intelligence-driven clinical decision support systems for early detection and precision therapy in oral cancer: a mini review. Frontiers in Oral Health. 2025; 6: 1592428.

[2] Ramesh E, Ganesan A, Lakshmi KC, Natarajan PM. Artificial intelligence-based diagnosis of oral leukoplakia using deep convolutional neural networks Xception and MobileNet-v2. Frontiers in Oral Health. 2025; 6: 1414524.
[3] Ganesan A, Kumar NG, Natarajan PM. Anticancer activity of silver nanoparticles synthesized from aqueous leaf extract of Solanum trilobatum (Purple fruit pea eggplant) on human oral cancer cells. Journal of Herbmed Pharmacololgy. 2024; 13(2): 260-268.
[4] Natarajan PM, Swamikannu B, Sivaraman NM, Stylin AGSQ. Prevention of Oral Cancer: A Comprehensive Guide. Journal of Pharmacy and Bioallied Sciences. 2024; 16(5): S4239-S4241.
[5] Umapathy V, Dhanavel A, Kesavan R, Natarajan PM, Bhuminathan S, Vijayalakshmi P. Anticancer Potential of the Principal Constituent of Piper nigrum, Piperine: A Comprehensive Review. Cureus. 2024; 16(2): e54425.
[6] Umapathy VR, Swamikannu B, Natarajan PM, Devi R, Nandini MS, Vimalarani, Vijayalakshmi P. In Silico Molecular Docking of Ocimum sanctum Phytochemicals: Targeting Key Biomarkers in Oral Cancer. Journal of Pharmacy and Bioallied Sciences. 2024; 16(5): S4792-S4799.
[7] Natarajan PM, Bhuminathan S, Rajan R, Bindu K, Loganathan K, Veerakumar R. The Crucial Role of Smoking Cessation in Preventing Oral Cancer. Journal of Pharmacy and Bioallied Sciences. 2024; 16(5): S4245-S4247.
[8] Swamikannu B, Umapathy VR, Natarajan PM, Nandini MS, Stylin AGSQ, Vimalarani V, Rajinikanth S. Unlocking the Therapeutic Benefits of Artemisia Annua: A Comprehensive Overview of its Medicinal Properties. Journal of Pharmacy and Bioallied Sciences. 2024; 16(5): S4248-S4253.
[9] Shree P, Sivaramakrishnan R, Kanniappan GV, Pandurangan V, Jayaraman S, Dhayalan VK, Mironescu M, Mironescu ID, Palanisamy CP. Antioxidant and biocompatible CuO-starch/PVA nanoscaffolds via ultrasonic green synthesis using Turbinaria conoides (brown marine macroalgae). Medicine in Drug Discovery. 2025; 28: 100238.
[10] Gong J, Lin J, Guan T, Pei J, Palanisamy CP, El-AtyFrom AMA. selenium tolerance to nanoplastic antagonism: Comprehensive characterization of L. casei SNUT1 and its extracellular vesicle–nanoselenium complex. Food Bioscience. 2025; 74: 107749.
[11] Poochi SP, Sundarraj R, Raju MV, Chandrasekaran MK, Ahalliya RM, Palanisamy CP, Kanniappan GV, Kondapavuluri BK, Thiruvengadam M. Harnessing Nature: Computational and Experimental Insights Into *Ipomoea obscura* Metabolites for Bladder Cancer Therapy. Chemistry and Biodiversity. 2025; 0: e00909.
[12] Dugganaboyana GK, Kannankumar MKG, Shivaramakrishna S, Raju MV, Chandrasekaran MK, Ahalliya RM, Panneerselvam N, Palanisamy CP, Kanniappan GV. Phytochemical insights, antioxidant activity and therapeutic potential of Cassia senna against prostate cancer in Wistar albino rats. Discover Applied Sciences. 2025; 7:1206.
[13] Natarajan SR, Krishnamoorthy R, Alshuniaber MA, Gatasheh MK, Rajagopal P, Veeraraghavan VP, Palanisamy CP, Jayaraman S. KDM1A Facilitates Oncogenic Potential in Colorectal Cancer Progression Through the Activation of AXIN/GSK3β/β-Catenin Signaling Pathways: Evidence From Integrated Transcriptomics and In Vitro Studies. The Journal of Gene Medicine. 2025; 27(11): e70053.
[14] Guan T, Gong J, Lin J, Palanisamy CP, Jinjin Pei J, El-Aty AMA. Machine learning-driven multimodal optimization of selenium biotransformation and flavor profiling in fermented apple–Yacon functional beverages. Innovative Food Science & Emerging Technologies. 2025; 105: 104198.
[15] Natarajan SR, Krishnamoorthy R, Alshuniaber MA, Alsulami TS, Gatasheh MK, Rajagopal P, Palanisamy CP, Govindan R, Veeraraghavan VP, Jayaraman S. ABCE1 facilitates tumour progression via aerobic glycolysis and inhibits cell death in human colorectal cancer cells through the p53 signalling pathway. Scientific Reports. 2025; 15: 24674.
[16] Huang Y, Guo H, Liu Y, Jin W, Palanisamy CP, Pei J, Oz F, El-Aty AMA. Effects of Natural Polysaccharides on the Gut Microbiota Related to Human Metabolic Health. Molecular Nutrition & Food Research. 2025; 69:e202400792.
[17] Poornima K, Meenakshi K.C, Manikandan V.R, Shankari G, Prabhu D, Rathi M.A, Palanisamy CP, Balaji R, Gopalakrishnan V.K. Exploring the anticancer potential of Jerantinine A from *Tabernaemontana coronaria* against prostate, breast, and ovarian cancers: A computational approach. *Journal of Complementary and Integrative Medicine*, 2025 22(2): 363–372.
[18] Palanisamy CP, Poompradub S, Sansanaphongpricha K, Jayaraman S, Subramani K. Faridah Sonsudin gGreen synthesis of Nigella sativa-mediated silver nanoparticles for enhanced antibacterial activity and wound healing: Mechanistic insights and biomedical applications. Environmental Nanotechnology, Monitoring & Management. 2025; 24: 101085.
[19] Surendran N, Raju MV, Chandrasekaran MK, Ahalliya RM, Palanisamy CP, Chandrasekaran G, Kanniappan GV. Physicochemical characterization of starch from Maranta arundinacea L.(arrowroot) rhizomes and its inhibition of COX-2: In vivo validation. Bioactive Carbohydrates and Dietary Fibre. 2025; 33: 100465.
[20] Kannappan P, Chandrasekaran MK, Raju MV, Gopalakrishnan S, Dhamodharan P, Ahalliya RM, Palanisamy CP, Raju B, Kanniappan GV. Exploring the anticancer potential of Jerantinine A from Tabernaemontana coronaria against prostate, breast, and ovarian cancers: a computational approach. Journal of Complementary and Integrative Medicine. 2025; 22(02): 363-372.

[21] Pei J, Kumarasamy RV, Jayaraman S, Kanniappan GV, Long Q, Palanisamy CP. Quercetin-functionalized nanomaterials: Innovative therapeutic avenues for Alzheimer's disease management. Ageing Research Reviews. 2025; 104: 102665.
[22] Jayaraman S, Prasad M, Natarajan SR, Krishnamoorthy R, Alshuniaber MA, Gatasheh MK, Veeraraghavan VP, Rajagopal P, Palanisamy CP. Molecular mechanisms underlying the effects of beta-sitosterol on TGF-β1/Nrf2/SIRT1/p53-mediated signaling in the kidney of a high-fat diet and sucrose-induced type-2 diabetic rat. Chemico-Biological Interactions. 2025; 411: 111443.
[23] Huang Y, Guo H, Liu Y, Jin W, Palanisamy CP, Pei J, Oz F, El-Aty AMA. Effects of Natural Polysaccharides on the Gut Microbiota Related to Human Metabolic Health. Molecular Nutrition & Food Research. 2025; e202400792.
[24] Prabhakaran P, Palanisamy CP, Shanmugam A, Damodharan P, Swaminathan H, Devaraj D, Ahalliya RM, Kanniappan GV. Isolation, structural characterization, and molecular docking studies on the bioactive compound from n-Hexane extract of Emilia sonchifolia (L.) DC against the pancreatic cancer target Aurora 2 Kinase. Journal of Complementary and Integrative Medicine. 2024; 22(1): 0290.
[25] Jiang H, Kumarasamy RV, Pei J, Raju K, Kanniappan GV, Palanisamy CP. Integrating engineered nanomaterials with extracellular vesicles: Advancing targeted drug delivery and biomedical applications. Frontiers in Nanotechnology. 2024; 6: 1513683.
[26] Guo H, Liu Y, Wan T, Song D, Palanisamy CP, Geng J, Pei J, Özmen S, El-Aty AMA. Toward personalized cancer management: Role of precision nutrition–diet interventions. Journal of Functional Foods. 2024; 123: 106584.
[27] Natarajan SR, Krishnamoorthy R, Alshuniaber MA, Al-Anazi KM, Farah MA, Rajagopal P, Palanisamy CP, Veeraraghavan VP, Jayaraman S. Identification of FOXM1 as a novel protein biomarker and therapeutic target for colorectal cancer progression: Evidence from immune infiltration and bioinformatic analyses. International Journal of Biological Macromolecules. 282 (Part 4): 137201.
[28] Rajendran MS, Jayaraman S, Khan JM, Jasmine S, Prabhakaran RK, Raju MV, Chandrasekaran MK, Ahalliya RM, Kannappan P, Palanisamy CP, Kanniappan GV. Investigating the colon toxicity and carcinogenic role of monosodium glutamate compared with Dimethylhydrazine in male Wistar rats: Exploring the link to childhood colon cancer risk. Journal of King Saud University - Science. 2024; 36(11): 103507.
[29] Kumarasamy RV, Natarajan P, Umapathy VR, Roy JR, Rab SO, Saeed M, Panagal M, Mironescu M, Srinivasan GP, Palanisamy CP. Clinical Applications and Therapeutic Potentials of Advanced Nanoparticles: A Comprehensive Review on Completed Human Clinical Trials. Frontiers in Nanotechnology. 2024; 6:1479993.
[30] Jin W, Pei JJ, Roy JR, Jayaraman S, Ahalliya RM, Kanniappan GV, Mironescu M, Palanisamy CP. Comprehensive review on single-cell RNA sequencing: A new frontier in Alzheimer's disease research. Ageing Research Reviews. 2024; 274: 102454.
[31] Pei J, Palanisamy CP, Jayaraman S, Natarajan PM, Umapathy VR, Roy JR, Panagal M, Jayaraman S. Curcumin-loaded polymeric nanomaterials as a novel therapeutic strategy for Alzheimer's disease: A comprehensive review. Ageing Research Reviews. 2024; 99: 102393.
[32] Pei J, Palanisamy CP, Jayaraman S, Natarajan PM, Umapathy VR, Roy JR, Thalamati D, Ahalliya RM, Kanniappan GV, Mironescu M. A comprehensive review on starch-based Sustainable Edible Films Loaded with Bioactive Components for Food Packaging. International Journal of Biological macromolecules. 2024; 274 (Part-1): 133332.
[33] Palanisamy CP, poompradub S, Sansanaphongpricha K, Subramani K, Sonsudin F. Increased expression levels of PDGF and VEGF magnify the wound healing potential facilitated by biogenic synthesis of silver nanoparticles. Nano-Structures & Nano-Objects. 2024; 39: 101236.
[34] Pei J, Palanisamy CP, Jayaraman S, Natarajan PM, Umapathy VR, Roy JR, Thalamati D, Ahalliya RM, Kanniappan GV, Mironescu M. Proteomics Profiling of Extracellular Vesicle for Identification of Potential Biomarkers in Alzheimer's Disease: A Comprehensive Review. Ageing Research Reviews. 2024; 99: 102359.
[35] Xi J, Wang T, Xian P, Liu X, Du M, Yang H, Palanisamy CP, Lin W, Long Q. Proteomic insights uncover enhanced neurotherapeutic potential in conditioned mesenchymal stem cell-derived extracellular vesicles. Extracellular Vesicle. 2024; 3: 100037.
[36] Pei J, Natarajan PM, Umapathy VR, Swamikannu B, Sivaraman NM, Krishnasamy L, Palanisamy CP. Advancements in the synthesis and functionalization of zinc oxide-based nanomaterials for enhanced oral cancer therapy. Molecules. 2024; 29(11): 2706.
[37] Gatasheh MK, Natarajan SR, Krishnamoorthy R, Alsulami TS, Rajagopal P, Palanisamy CP, Veeraraghavan VP, Jayaraman S. Molecular analysis to identify novel potential biomarkers as drug targets in colorectal cancer therapy: an integrated bioinformatics analysis. Molecular and Cellular Oncology. 2024; 11(1): 2326699.
[38] Pei J, Yan Y, Jayaraman S, Rajagopal P, Natarajan PM, Umapathy VR, Gopathy S, Roy JR, Sadagopan CS, Thalamati D, Palanisamy CP, Mironescu M. A review on advancements in the application of starch-based nanomaterials in biomedicine: Precision drug delivery and cancer therapy. International Journal of Biological Macromolecules. 2024; 130746.
[39] Pei JJ, Yan Y, Palanisamy CP, Jayaraman S, Natarajan PM, Umapathy VR, Gopathy S, Roy JR, Sadagopan JC, Thalamati D, Mironescu M. Materials-based drug delivery approaches: Recent advances and future perspectives. Green Processing and Synthesis. 2024; 13: 20230094.

[40] Pei JJ, Deng W, Liu Y, Guo Y, Chen J, Abdu H, Khan MR, Palanisamy CP, El-Aty AM. A Comprehensive Review of Cornus officinalis: Health Benefits, Phytochemistry, and Pharmacological Effects for Functional Drug and Food Development. Frontiers in Nutrition. 2023; 10: 1309963.
[41] Alugoju P, Palanisamy CP, Anthikapalli NVA, Jayaraman S, Prasanskulab A, Chuchawankul S, Dyavaiah M, Tencomnao T. Exploring the anti-aging potential of natural products and plant extracts in budding yeast Saccharomyces cerevisiae: A review. F1000Research. 2023; 12: 1265.
[42] Lavanya M, Krishnamoorthy R, Alshuniaber MA, Manoharadas S, Palanisamy CP, Veeraraghavan VP, Jayaraman S, Rajagopal P, Padmini R. Formulation, characterization and evaluation of gelatin-syringic acid/zinc oxide nanocomposite for its effective anticancer, antioxidant and anti-inflammatory activities. Journal of King Saud University-Science. 2023; 35: 102909.
[43] Palanisamy CP, Poompradub S, Sansanaphongpricha K, Jayaraman S, Subramani K, Sonsudin F. Biosynthesis of silver nanoparticles (AgNPs) using ethanolic extract of Nigella sativa (L.) seeds promotes wound healing via PDGF and VEGF signalling pathways activation. Biocatalysis and Agricultural Biotechnology. 2023; 54: 102970.
[44] Prasad M, Jayaraman S, Natarajan SR, Veeraraghavan VP, Krishnamoorthy R, Gatasheh MK, Palanisamy CP, Elrobh M. Piperine modulates IR/Akt/GLUT4 pathways to mitigate insulin resistance: Evidence from animal and computational studies. International Journal of Biological Macromolecules. 2023; 253: 127242.
[45] Palanisamy CP, Pei JJ, Phaniendra A, Venkata AAN, Jayaraman S, Veeraragahavan VP, Sridevi G, Roy JR, Janaki CS, Thalamati D, Mironescu M, Luo Q, Chai Y, Long Q. New Strategy of Neurodegenerative Disease Treatment with Extracellular Vesicles (EVs) Derived from Mesenchymal Stem Cells (MSCs). *Theranostics*. 2023; 13(12):4138-4165. doi:10.7150/thno.83066.
[46] Palanisamy CP, Phaniendra A, Jayaraman S, Poompradub S. *Nigella sativa* L. seed extracts promotes wound healing progress by activating VEGF and PDGF signalling pathways: *An in vitro* and *in silico* study. *F1000 Research*. 2023; 12: 436.
[47] Natarajan PM, Umapathy VR, Murali A, Swamikannu B. (2022). Computational Simulations of Identified marine-derived Natural Bioactive Compounds As Potential Inhibitors of Oral Cancer. Future Science OA. 2022; 8(3).
[48] Natarajan PM, Umapathy VR. Role of transcriptomics in the study of oral cancer. Frontiers in Oral Health. 2025; 6:1524364.
[49] Vidhyarekha U, Natarajan PM, Bhuminathan S, Sabarinathan J, Suba R, Vijayalakshmi P. Role of artificial intelligence in Oral Cancer. Advances in Public Health. 2024. 2024: 3664408.
[50] Ganesan A, Kumar NG, Natarajan PM, Gauthaman J. Automated classification of elongated styloid processes using deep learning models-an artificial intelligence diagnostics. Frontiers in Oral Health. 2025; 5: 1424840.
[51] Umapathy VR, Natarajan PM, Swamikannu B. Regenerative Strategies in Dentistry: Harnessing Stem Cells, Biomaterials and Bioactive Materials for Tissue Repair. Biomolecules. 2025; 15: 546.
[52] Natarajan PM. Dental Bioinformnatics-Current Scope and Future perspectives. Research Journal of Pharmacy and Technology. 2022;15(5):2351-6.
[53] Ganesan A, Kumar NG, Natarajan PM. Solanum trilobatum leaf extract-derived silver nanoparticles downregulate the PI3K/AKT/mTOR signaling pathway and attenuate oral squamous cell carcinoma cell proliferation. Journal of Herbmed Pharmacology. 2024; 13(2): 300-307.
[54] Pei JJ, Perumal NC, Meng P, Long Q, Palanisamy CP. AI-assisted FTIR spectroscopic profiling of exosomes: Emerging frontiers in early detection of Alzheimer's disease. Ageing Research Reviews. 2026; 103311.
[55] Raja FSD, Abraham L, Rangasamy K, Saikia K, Rathankumar AK, Mironescu M, Mironescu I, Palanisamy CP, Kanniappan GV. Next-Generation Microbiome Therapeutics: Psychobiotics and Fecal Microbiota Transplants (FMT) for Mental Health Treatment. Frontiers in Cellular and Infection Microbiology. 2026; 16: 1719357.
[56] Subramani K, Srinivasan S, Shanmugam P, Palanisamy CP, Sonsudin F, Poompradub S. Sustainable phytochemical mediated-ZnO nanoparticles derived from Crescentia cujete for toxicological evaluation and multifunctional environmental applications. Environmental Nanotechnology, Monitoring & Management. 2026; 26: 101180.
[57] Kunamalla RP, Panagal M, Palanisamy CP. Green-engineered multiscale starch/PVA nanofibrous scaffolds embedded with CuO nanoparticles from Sargassum ilicifolium for potent antimicrobial performance. Genetics and Molecular Research. 2026; 25(13s): 1-9.
[58] Dharmaprakash S, Gunasekaran VP, Sivaramakrishnan R, Kanniappan GV, Jayaraman S, Mironescu M, Rajabathar JR, Mironescu ID, Palanisamy CP. Marine macroalgae-mediated ultrasonic-assisted green synthesis of CuO nanoparticles embedded in starch/PVA electrospun nanoscaffolds for in vitro α-amylase and α-glucosidase inhibitory activity. Scientific Reports. 2026; 16: 26243.
[59] Surendran N, Chandrasekaran G, Raju MV, Chandrasekaran MK, Ahalliya RM, Palanisamy CP, Kanniappan GV, Arcot R, Alharbi NS, Thiruvengadam M. Anti-inflammatory potential of ethanolic extract of Maranta arundinacea L.: Insights from COX-2 modulation and oxidative stress analysis. South African Journal of Botany. 2026; 195: 142-151.

[60] Pei J, Senthilkumar MV, Hessini K, Subramaniyam S, Sivaramakrishnan R, Kanniappan GV, Jayaraman S, Palanisamy CP. Green fabrication of starch/PVA/CuO nanoscaffolds using marine macroalgae extract for enhanced anti-inflammatory activity. Sustainable Chemistry and Pharmacy. 2026; 51: 102397.
[61] Balasubramanian V, Loganathan L, Muthuswamy K, Viswanathan TM, Raju MV, Chandrasekaran MK, Ahalliya RM, Poorasamy J, Palanisamy CP, Dominic S, Kanniappan GV. Anticancer therapeutic efficacy of PEGylated β-galactosidase from Aspergillus terreus in DMBA-induced breast cancer: Toxicological, molecular and histopathological evaluation in Wistar rats. International Journal of Biological Macromolecules. 2026; 360: 151856.
[62] Jayaraman S, Eswaran A, Rajagopal P, Palanisamy CP, Veerakumar P, Veeraraghavan VP, Sirasanagandla SR. Neuroendocrine-associated epigenetic factors in cellular senescence: mechanisms and therapeutic implications. Biogerontology. 2026; 27(2): 64.
[63] Ponnusamy B, Rajagopal P, Palanisamy CP, Veeraraghavan VP, Jayaraman S. Mechanistic Exploration of the anticancer activity of Justicia adhatoda Plant Leaf Ethanolic Extract against Colon Cancer Cells: An in silico and in vitro Approach. Asian Pacific Journal of Cancer Prevention. 2026; 27(3): 1069-1080.
[64] Pei J, Saran VS, Sivaramakrishnan R, Kanniappan GV, Pandurangan V, Jayaraman S, Dhayalan VK, Mironescu M, Mironescu ID, Palanisamy CP. Ultrasonic-assisted, Sargassum ilicifolium (brown marine macroalgae)-mediated biogenic synthesis of CuO nanoparticles incorporated in starch/PVA electrospun nanoscaffolds: In vitro safety and antioxidant efficacy assessment. Bioorganic Chemistry. 2026; 173: 109679.
[65] Raj MAPA, Subramaniyam S, Kanniappan GV, Jayaraman S, Palanisamy CP. Sustainable fabrication of starch/PVA/CuO electrospun nanoscaffolds from Turbinaria ornata (marine macroalgae) extract: Physicochemical characterization and antidiabetic evaluation. Kuwait Journal of Science. 2026; 53(2): 100545.
[66] Pei J, Ganesh NS, Subramaniyam S, Sivaramakrishnan R, Kanniappan GV, Jayaraman S, Palanisamy CP. Sustainable fabrication of starch/PVA/CuO electrospun nanoscaffolds from Padina tetrastromatica (Brown macroalgae) extract: Physicochemical characterization and antidiabetic assessment. Sustainable Chemistry One World. 2026; 9: 100195.
[67] Sakthiraj A, Sivaramakrishnan R, Subramaniyam S, Kanniappan GV, Pandurangan V, Jayaraman S, Dhayalan VK, Mironescu M, Mironescu ID, Palanisamy CP. Starch/PVA electrospun nanoscaffolds loaded with ultrasonic-assisted green-synthesis of CuO nanoparticles from marine macroalgae (Gracilaria corticata) extract: Cytotoxicity and antioxidant analysis. Chemical Physics Impact. 2026; 12: 101018.
[68] Raju M, Chandrasekaran MK, Loganathan L, Ahalliya RM, Mironescu M, Mironescu ID, Palanisamy CP, Kanniappan GV. Lipid remodeling and ferroptosis in phosphatidylcholine-mediated tumor–stroma crosstalk. Frontiers in Molecular Biosciences. 2026; 13: 1742305.
[69] Kunamalla R, Panagal M, Palanisamy CP. Biogenic synthesis and fabrication of starch/PVA/CuO electrospun nanoscaffolds from Sargassum ilicifolium (brown marine macroalgae) extract for anticancer activity on HT-29 and MCF-7 cancer cells. Biocatalysis and Agricultural Biotechnology. 2026; 72: 103923.
[70] Pei J, Govindaraj H, Sivaramakrishnan R, Kanniappan GV, Pandurangan V, Dhayalan VK, Mironescu M, Mironescu ID, Jayaraman S, Palanisamy PC. Sustainable fabrication of biopolymer-based (starch/PVA) nanoscaffolds loaded with green-synthesized CuO nanoparticles from Sargassum wightii (marine macroalgae): Cytocompatibility and antioxidant activity. Biomaterials Advances. 2026; 182: 214660.
[71] Pei J, Perumal NC, Meng P, Long Q, Palanisamy CP. Extracellular vesicle-based biosensors for Alzheimer's disease: A new frontier in precision diagnostics. Ageing Research Reviews. 2026; 113: 102904.
[72] Natarajan PM. Computational Studies on Recent Congeners of Fluoroquinolones and Nitroimidazoles for Their Use in Periodontal Therapy. Journal of Pharmacy and Bioallied Sciences. 2024; 16(5): S4731-S4740.
[73] Yadalam PK, Arumuganainar D, Natarajan PM, Ardila CM. Artificial intelligence-powered prediction of AIM-2 inflammasome sequences using transformers and graph attention networks in periodontal inflammation. Scientific Reports. 2025; 15: 8733.
[74] Yadalam PK, Chatterjee S, Natarajan PM, Ardila CM. Comparison of light gradient boosting and logistic r egression for interactomic hub genes in Porphyromonas gingivalis and Fusobacterium nucleatum-induced perio dontitis with Alzheimer's disease. Frontiers in Oral Health. 2025; 6:1463458.
[75] Natarajan PM, Bhuminathan S, Leela B, Bindu K, Loganathan K, Ramachandran V. Smoking and its Role in Oral Cancer. Journal of Pharmacy and Bioallied Sciences 16(5): S4242-S4244.
[76] Yadalam PK, Natarajan PM, Ardila CM. Variational graph autoencoder for reconstructed transcriptomic data associated with NLRP3 mediated pyroptosis in periodontitis. Scientific Reports. 2025; 15: 1962.
[77] Pei JJ, Palanisamy CP, Phaniendra A, Venkata AAN, Natarajan PM, Umapathy VR, Swamikannu B, Jayaraman S, Rajagopal P, Poompradub S. A comprehensive review on bio-based materials for chronic diabetic wounds. *Molecules*. 2022; 28(2), 604.
[78] Palanisamy CP, Cui B, Zhang H, Gunasekaran VP, Ariyo A, Jayaraman S, Veeraraghavan V, Rajagopal P. A critical review on starch-based electrospun nanofibrous scaffolds for wound healing application. International Journal of Biological Macromolecules. 2022; 222 (Part: B): 1852-1860.
[79] Monisha P, Ponnulakshmi R, Nalini D, Vishnu P V, Palanisamy CP, Cui B, Shankargouda P, Selvaraj J. A comprehensive review on high fat diet-induced diabetes mellitus: An epigenetic view. The Journal of Nutritional Biochemistry. 2022; 2022: 109037.